11068 Session
2022 A3 – Transmission and Distribution Equipment
PS 2 – Decarbonisation of Transmission and Distribution Equipment

Investigation of the Switching Behaviour, Voltage Distribution and Post-Arc Current of series-connected Vacuum Interrupter Units for Live Tank and Dead Tank Circuit Breakers ≥ 420 kV

Tobias GOEBELS*, Paul Gregor NIKOLIC, Radu-Marian CERNAT, Jan WEISKER, Stefan GIERE
Siemens Energy, Erlangen and Berlin
Germany
tobias.goebels@siemens-energy.com

SUMMARY

Circuit breakers are important operational elements with intrinsic safety function in electrical power grids all over the world. Due to the discussion about a phase-out of sulphur hexafluoride (SF_6) as insulating and arc quenching gas in high-voltage switchgear applications for new installations within the next decades, the investigation of various SF_6-alternatives is even more in the focus of sciences' and industry's current research and development efforts.
In this context, vacuum switching technology combined with a Clean Air (80% N_2 and 20% O_2) insulation represents an environment-friendly (GWP = 0), maintenance free and highly performant SF_6-free solution for future high-voltage switchgear applications as it already does for voltages up to U_r = 170 kV today. Nevertheless, due to the nonlinearly increasing dielectric strength of vacuum it does not seem to be possible to develop single-break vacuum interrupter units for the higher voltage levels with $U_r \geq$ 420 kV with a technically and economically justifiable effort. Therefore, series connections of several high-voltage vacuum interrupter units must also be considered as a solution and are being investigated and presented in this contribution.
In contrast to previously presented results [1] additional current and voltage probes are applied during high-power tests to enable a measurement of the post-arc currents of the vacuum interrupter gaps after current zero and analyse their effect on the voltage distribution of series-connected vacuum interrupter units. Moreover, a field sensor is used to measure the voltage distribution noninvasively in contrast to connecting voltage dividers with significant capacitance values.

KEYWORDS

Vacuum switching technology, series-connected vacuum interrupter units, high-voltage circuit breaker, post-arc current, voltage distribution, Clean Air insulation

1 INTRODUCTION

High-voltage circuit breakers are operational elements with intrinsic safety function in electrical power grids all over the world. Today, more and more countries and companies worldwide commit themselves to reduce CO_2 emissions and even bring them down to zero [2]. In this regard, the revisions of global regulations, such as the Californian (CARB) regulation for reducing greenhouse gases (GHG) in gas-insulated equipment and the review of the European regulation on fluorinated gases, discuss and propose a phase-out of SF_6 as insulating and switching gas in high-voltage applications for new installations within the next decades. Moreover, there is an increasing focus of grid operators to install climate-neutral equipment without GHG-emissions during operation and at end-of-life within their assets. Thus, the investigation and evaluation of various SF_6-alternatives is even more in the focus of sciences' and industry's current research and development efforts.
Vacuum switching technology in combination with a Clean Air insulation with zero emissions yields an environment-friendly, maintenance free and highly performant SF_6-free solution for future high-voltage switchgear. For rated voltages up to $U_r = 170$ kV single-break vacuum interrupter units (VIUs) are already commercially available, for rated voltages up to $U_r = 245$ kV they are under development [3]. The advantages of and experiences with Clean Air insulation and vacuum interrupters are described in detail in [4, 5]. Due to the nonlinearly increasing dielectric strength of vacuum it is hard to imagine developing single-break vacuum interrupter units for $U_r \geq 420$ kV with a technically and economically justifiable effort. Therefore, series connections of two or more high-voltage vacuum interrupter units are being investigated. One of the main challenges for the successful application of these series connections is the symmetrical voltage distribution across the interrupter units [6, 7].
In contrast to other available publications where mostly either theoretical or practical studies regarding series connections of partially larger numbers of medium-voltage vacuum interrupter units are presented [8-12], in this contribution the relevant aspects are investigated by means of laboratory prototypes using high-voltage vacuum interrupter units.

2 POST-ARC CURRENT

For using vacuum switching technology for rated voltages up to $U_r = 420$ kV and beyond multiple break concepts are under consideration. This principle can e.g. be used for metal-enclosed and live tank circuit breakers whereby the realization of compact equipment in Clean Air requires an adaption of the known switchgear design due to (among others) different contact gaps and opening velocity of vacuum circuit breakers compared to gas-filled ones. In addition, a lower dielectric strength of Clean Air compared to SF_6 also has to be considered (cf. figure 1).

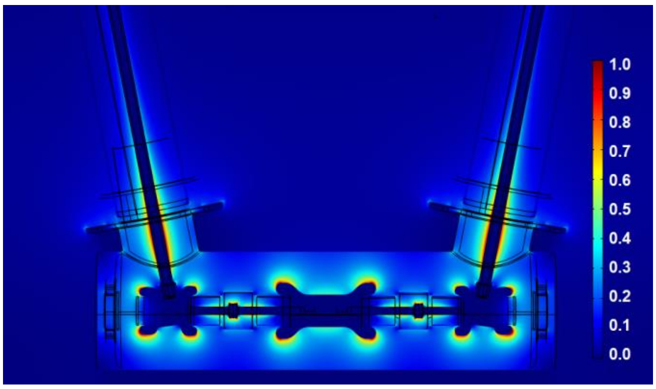

Figure 1: Electric field distribution [p.u.] of possible series connection of two vacuum interrupter units in a metal-enclosed circuit breaker

In this context, it also must be taken into account that the post-arc current (i_{PA}) of vacuum interrupter units differs from the one of SF_6 interrupter units [13-17].
Thus, to develop reliable and sustainable switchgear, the required grading capacitance needs to be known related to the resulting switching performance over the whole value range. In preceding investigations, the principle of a double breaking circuit breaker based on vacuum interrupter units as switching elements and Clean Air as insulation medium is successfully demonstrated on the example of a live tank circuit breaker [1].
At the same time, further investigations are ongoing. This is necessary due to the physical processes coming along with the current interruption process. The physical mechanisms for arc interruption are different comparing vacuum and gas-filled circuit breakers. On the one hand, the interruption process in vacuum interrupter units is strongly dependent on the electron and ion current density resulting from the metal vapor in the vacuum gap. On the other hand, the successful current interruption in gas-filled circuit breakers depends on the recombination of charge carriers of the plasma in the gas gap. Additionally, both switching principles yield different contact distance, contact shape and contact materials, as well as a different electrical field distribution in the contact gap.
Resulting from all these effects, the post-arc current in a vacuum interrupter unit is higher than in an SF_6 interrupter unit (several 10 to several 100 Milliamperes for SF_6 vs. several Amperes to few 10 Amperes for vacuum [13-17]) and thus has a higher influence on the potential distribution and the resulting electrical field inside the VIU during the transient recovery voltage phase. To point out the influence the post-arc current has on the potential distribution the equivalent circuit diagram shown in figure 2 is used. Here, only the relevant elements for the potential distribution are depicted.

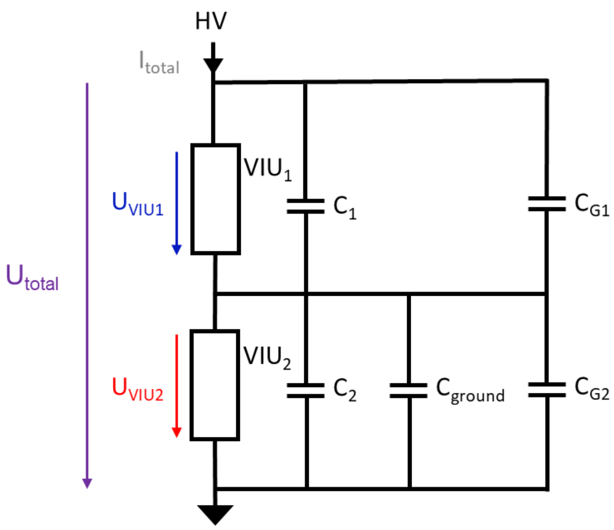

Figure 2: Simplified equivalent circuit diagram of series connection of two VIUs with grading capacitors (cf. [1])

For describing the voltage distribution, a parameter ΔU is introduced. It can be described using the following formula:

$$\Delta U = U_{VIU1} - U_{VIU2} \tag{1}$$

With $Q = C \cdot U$ it can be written as:

$$\Delta U = \frac{q(C_1 + C_{G1})}{C_1 + C_{G1}} - \frac{q(C_2 + C_{G2} + C_{ground})}{C_2 + C_{G2} + C_{ground}} \quad (2)$$

Using $q(t) = \int_{t_0}^{t} i(t)dt$ leads to:

$$\Delta U = \frac{\int_{t_0}^{t} i(C_1 + C_{G1})dt}{C_1 + C_{G1}} - \frac{\int_{t_0}^{t} i(C_2 + C_{G2} + C_{ground})dt}{C_2 + C_{G2} + C_{ground}} \quad (3)$$

According to Kirchhoff's law: $i(C_1 + C_{G1}) - i\left(C_2 + C_{G2} + C_{ground}\right) = i_{PA2} - i_{PA1}$

In the test setup, grading capacitors with equal capacitances are used so that $C_{G1} = C_{G2} = C_G$. Moreover, the capacitance of the grading capacitors is by far larger than the simulated and calculated stray and earth capacitances of the setup (C_G = 900 pF vs. $C_1 \approx C_2 \approx C_{ground} \approx$ 20 pF). Therefore, the stray and earth capacitances can be neglected and finally the following formula is obtained:

$$\Delta U = \frac{\int_{t_0}^{t} (i_{PA2} - i_{PA1})dt}{C_G} \quad (4)$$

Thus, it can be seen that the voltage distribution has two main influencing factors, the grading capacitance and the post-arc currents, more precise the difference between the two post-arc currents. Also, it is obvious that a higher grading capacitance diminishes the influence of the post-arc currents.
Additional factors influencing the post-arc current to be considered are the arcing time, the amplitude and rate of rise di/dt of the short-circuit current and the rate of rise of the transient recovery voltage du/dt. Thermal effects may also play a vital role as a heated contact can emit more metal vapor leading to a higher post-arc charge due to more charge carriers in the contact gap. These effects are subject to ongoing investigations.

3 TEST SETUP

In continuation of preceding investigations, a test setup (cf. [1]) is equipped with additional measuring equipment to assess the post-arc current of the vacuum interrupter units as well as the charging currents of the connected grading capacitors. This measuring equipment can be applied to live tank as well as metal-enclosed circuit breakers to evaluate the relevant parameters of the switching operation. Measurements are performed during different test duties according to IEC 62271-101 with and without grading capacitors. Details of this test setup and the used measuring equipment are given in figures 3 and 4. The HV-Circuit shown in figure 4 in combination with the reactor L_{RV} is used to adapt the TRV-parameters (e.g. amplitude and rate of rise) to the predefined values according to the standard.

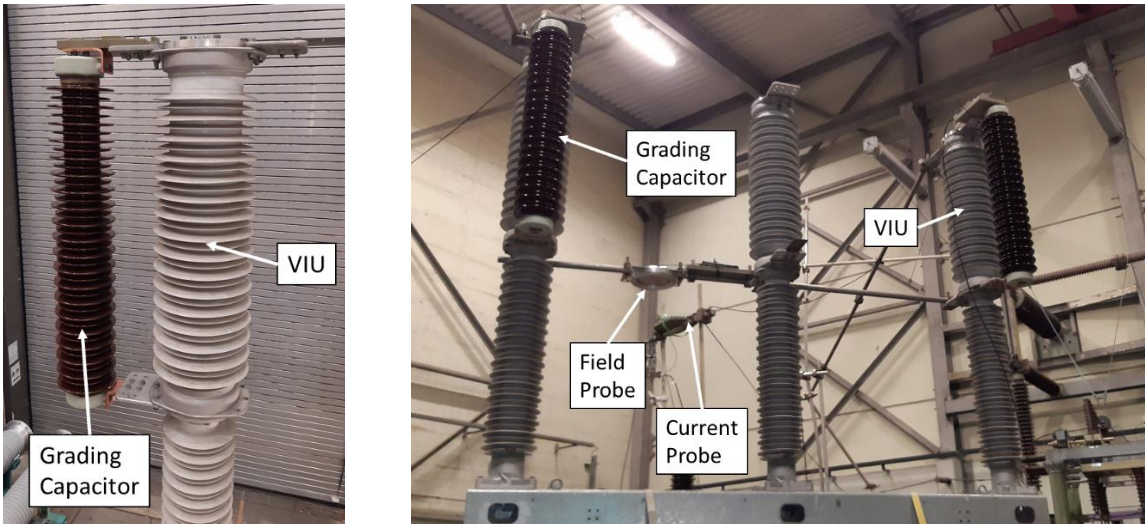

Figure 3: Test setup with grading capacitor connected in parallel to vacuum interrupter unit (VIU) (left) and test setup with field probe and current probe (right)

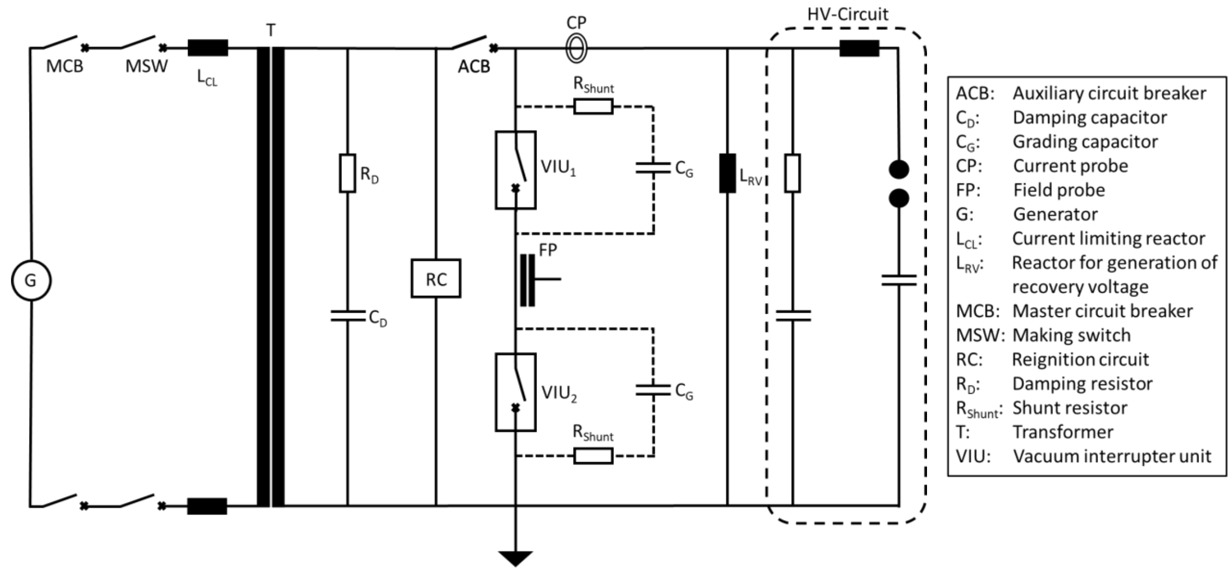

Figure 4: Equivalent circuit diagram with relevant components of test circuit and test setup

For the investigations two poles of a 145 kV live tank high-voltage vacuum circuit breaker are equipped with grading capacitors to simulate a series connection of vacuum interrupter units. The post-arc current is measured using a Pearson 110 current probe attached to the high-voltage injection circuit of the experimental setup. A field probe is used to measure the mid potential between both VIUs non-invasively. Measuring it with a common voltage divider would distort the voltage distribution due to the divider's input capacitance. In addition, current measuring shunt resistors are mounted on the grading capacitors' terminals to enable a measurement of the charging currents. The measuring signals are submitted by optically connected probes to avoid EMC interferences and for safety reasons.

4 MEASUREMENT RESULTS

Exemplary current zeros from asymmetrical and symmetrical tests with 100% of the rated short-circuit current (test duties T100a and T100s) including post-arc current measurement and the recovery voltage are given in figure 5.

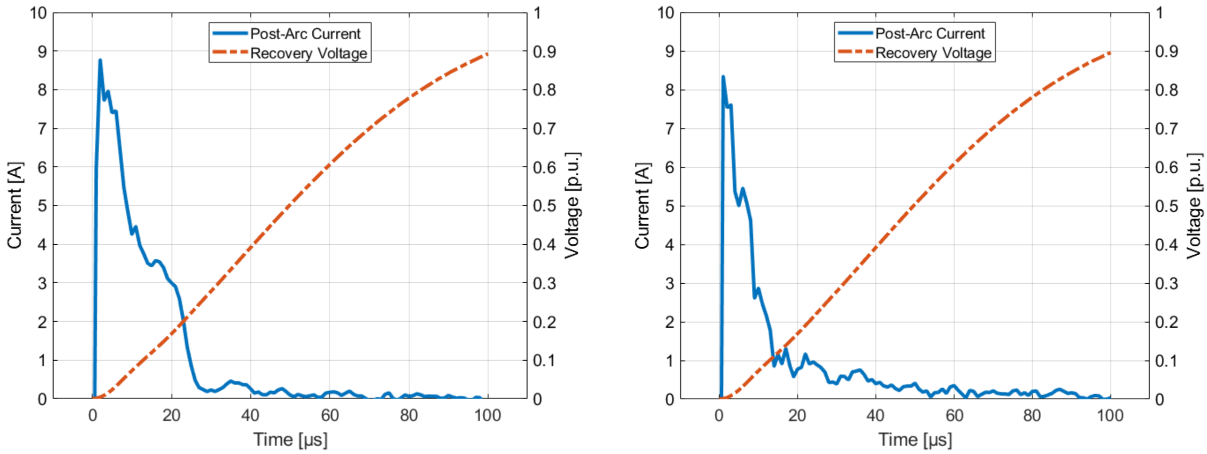

Figure 5: Exemplary post-arc current measurements from a T100a (left) and a T100s (right) test duty

The measurements show a post-arc current with a peak value of 8.4…8.9 A and a duration of approx. 15…25 µs, starting at instant ($t_1 = 0$ µs) with the rise of the transient recovery voltage. Besides peak value and duration the charge quantity is an important parameter to characterize the post-arc current. It can be calculated using the formula given in section 2. For the integration, a threshold current value of 1 A is chosen and the post-arc current is considered to have subsided when falling below this value for the first time. For the results of test duty T100a this leads to a post-arc time of $t_{2,a}$ =25 µs and a charge of Q_a = 103 µC. For T100s a time of $t_{2,s}$ = 14 µs is obtained leading to a charge of Q_s = 69 µC.
For the following tests, at first it is necessary to verify whether the field probe delivers correct measurement data. Therefore, the test setup with grading capacitors is used and the charging current of the capacitor connected in parallel to VIU_2 is integrated using the following formula:

$$u_c(t) = \frac{1}{C} \cdot \int_{t_0}^{t} i_c(t)dt \qquad (5)$$

As a result, the mid potential between both VIUs is obtained (the small voltage drop across the shunt resistor is neglected). In figure 6 on the left-hand side this calculated potential is compared to the potential measured by the field probe. A good degree of consistency can be observed. To verify the approach of integrating the capacitor’s charging current, also the charging current of the capacitor connected in parallel to VIU_1 is integrated and both calculated values are added up. The total voltage calculated like this provides almost perfect match with the value measured with a calibrated voltage divider connected to the high-voltage side, as also shown in the same diagram. Thus, the approach of integrating the charging currents is valid and the field probe can be used to measure the mid potential.
On the right-hand side of figure 6, the voltage distribution for a switching operation without connected grading capacitors is shown. Using the measured mid potential, a voltage distribution of 81% : 19% can be calculated.

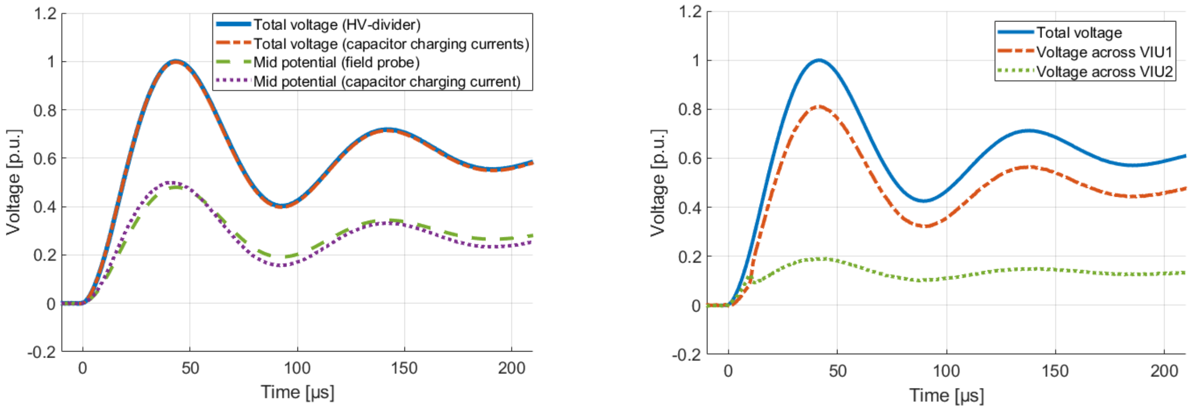

Figure 6: Left: Verification of measured values of the field probe; Right: Voltage distribution without grading capacitors

Additional investigations of the grading capacitor charging currents were performed with the test setup. The results for exemplary distributions of the charging currents with no significant influence and with a minor influence of the post-arc currents and the resulting voltage distributions are given in figures 7 and 8. Figure 9 yields an example with major influence of the post-arc currents on the charging currents and thus on the voltage distribution across the grading capacitors. This can e.g. be achieved by an artificially forced delayed opening of VIU_2 compared to VIU_1 realized by a modification of the operating mechanism (approx. 3 ms).
On the left-hand side of figures 7, 8 and 9 the charging currents of the grading capacitors are shown. It can be seen that they are in same value range as the post-arc currents presented in figure 5. On the right-hand side of these figures, the voltages of both capacitors are shown, calculated according to formula (5).
In figure 7 a voltage distribution of 51% : 49% is achieved while figure 8 shows a distribution of 55% : 45% and figure 9 of 70% : 30%. These differences in the voltage distributions result from the dissimilarity of the charging currents of the grading capacitors, which is strongly dependent on the post-arc current of the vacuum interrupter units. Due to the comparable amplitudes of post-arc current and charging currents of the grading capacitors this effect gains more importance when using series-connected vacuum interrupter units compared to previously used SF_6 interrupter units (cf. [13-17]).

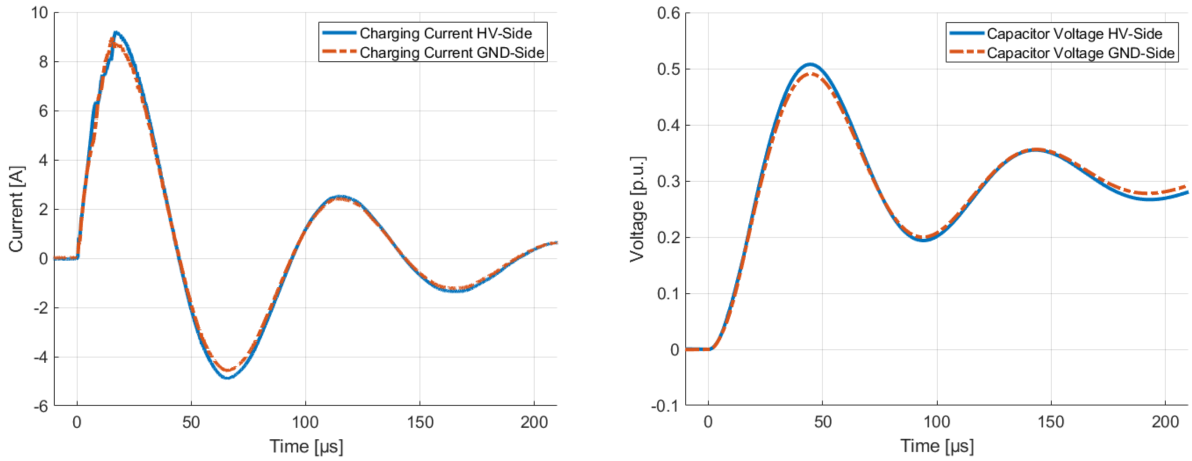

Figure 7: Exemplary voltage distribution across the grading capacitors for charging currents without significant influence of the post-arc currents

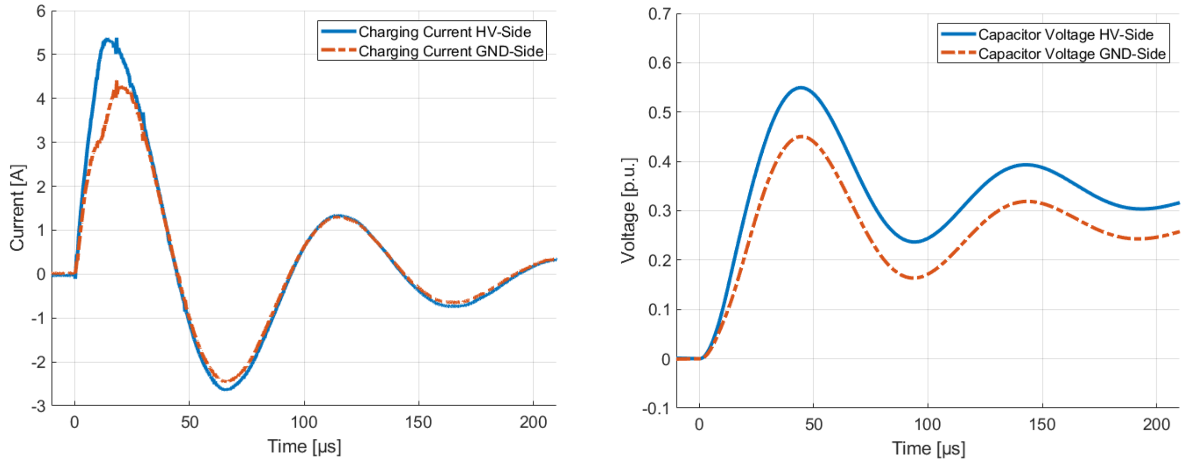

Figure 8: Exemplary voltage distribution across the grading capacitors for charging currents with minor influence of the post-arc currents

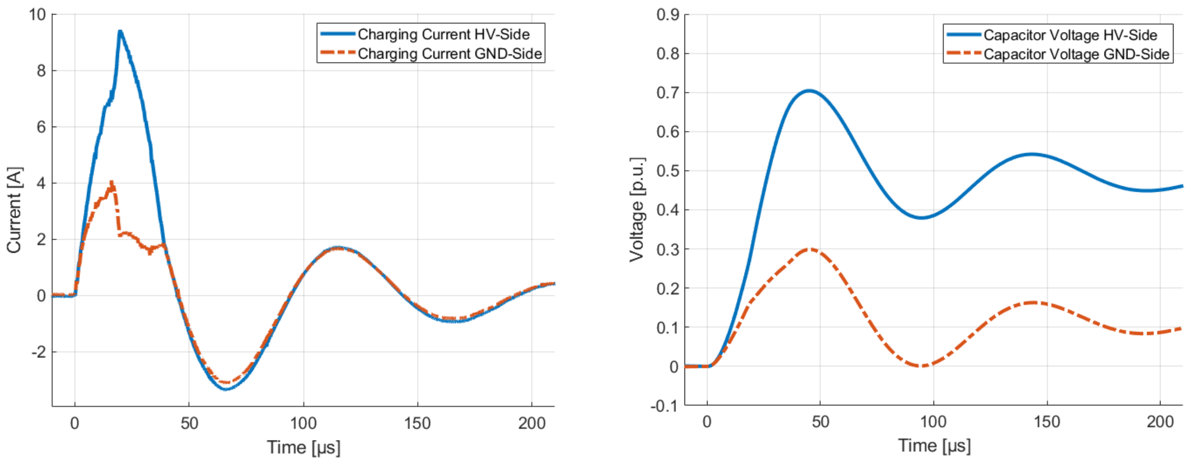

Figure 9: Exemplary voltage distribution across the grading capacitors for charging currents with major influence of the post-arc currents, e.g. forced by artificially delayed opening of VIU_2

The post-arc characteristics need to be considered when using grading capacitors with series-connected vacuum interrupter units as they can lead to inequalities of the charge of the grading capacitors and thus influence the voltage distribution. It is also shown in formula (4) that the post-arc currents do have a direct influence on the voltage distribution. This was also confirmed by simulations that were performed in prior to the experimental investigations.

The test results shown above confirm that an even voltage distribution results from symmetrical post-arc currents (and thus symmetrical charging currents of the grading capacitors). An artificially created delay between the contact opening moments of the VIUs leads to a significantly higher current through the grading capacitor connected in parallel to VIU_1 and thus provokes an uneven voltage distribution. In that case, more than two-thirds of the total voltage drop across the first grading capacitor and thus also across VIU_1.

5 CONCLUSION AND OUTLOOK

As presented in previous contributions it is necessary to equalize the voltage distribution over the vacuum interrupter units (e.g. with grading capacitors) when connecting them serially because otherwise stray capacitances can lead to an uneven voltage distribution. That could lead to a dielectric breakdown of the more stressed interrupter unit and thus to a following breakdown of the previously less stressed one. Nevertheless, it is not sufficient to only connect grading capacitors in parallel to the VIUs but also to understand when and how they are charged and how their charge is influenced by the post-arc currents of the vacuum interrupter units. Here, previous theoretical considerations are confirmed by measurements of the post-arc current and the charging currents of the grading capacitors. The results show that there is a direct link between post-arc current and voltage distribution on the one hand and post-arc current and charging currents (and thus voltages) of the grading capacitors on the other hand.
Research is being continued and more detailed investigations on the correlation between charging current of the capacitors, post-arc current and their effects on the series connection will be performed. A deep physical understanding of the processes coming along with the interruption process lays the basis for the successful realization of high-voltage switchgear with $U_r \geq 420$ kV based on (series-connected) vacuum interrupter units and Clean Air insulation.

Parts of the research work presented in this contribution were supported by the German Federal Ministry for Economic Affairs and Climate Action.

Supported by:

Federal Ministry
for Economic Affairs
and Climate Action

on the basis of a decision
by the German Bundestag

BIBLIOGRAPHY

[1] P. G. Nikolic, T. Goebels, J. Teichmann, J. Weisker, R. Huth: “Basic aspects of switching with series-connected vacuum interrupter units in high-voltage metal-enclosed and live tank arrangements”, 48th Cigré Session, A3-112, Paris, France, August 2020.

[2] D. Helbig, S. Bose, P. Gronbach, K. Juhre, M. Kuschel: “Transition to Climate Neutral, Safe and Sustainable Power Grids – Benefits for Society, Grid Operators and Manufacturers », Cigré Session 2022, ID: 1102, Paris, France, August 2022.

[3] M. Kuschel, D. Helbig, K. Kunde, S. Kosse, K. Pohlink, U. Prucker and J. Teichmann: “Entwicklungsstand, Vor-Ort-Erfahrungen und Ausblick zu SF_6-freien Hochspannungsschaltanlagen”, VDE-Hochspannungstechnik, Berlin, Germany, November 2020.

[4] P. Gronbach, K. Butter, A. Sarkar, A.-S. Mortensen, D. Collard, U. Prucker, M. Kasner: “Experience with F-gas-free High voltage equipment for On- and Offshore applications”, Cigré Session 2022, ID: 1069, Paris, France, August 2022.

[5] M. Kuschel, L.-V. Badicu, J. Christian, M. Kieper, K. Kunde, U. Prucker, J. Riedl: "World's first F-gas-free and climate neutral insulated 420 kV GIS busducts installation at Transnet BW", Cigré Session 2022, ID: 1082, Paris, France, August 2022.
[6] D. Huang, G. Wu, J. Ruan: "Study on Static and Dynamic Voltage Distribution Characteristics and Voltage Sharing Design of a 126-kV Modular Triple-Break Vacuum Circuit Breaker", IEEE Transactions on Plasma Science, Vol. 43, No. 8, August 2015, pp. 2694-2702.
[7] S. Shu, J. Ruan, D. Huang, G. Wu, C. Liu: "Study on Transient Recovery Voltage Distribution Mechanism and Grading Capacitor of Double-Break Vacuum Circuit Breaker", 25th International Symposium on Discharges and Electrical Insulation in Vacuum (ISDEIV), Tomsk, Russia, September 2012, pp. 501-504.
[8] X. Yu, F. Yang, X. Li, S. Ai, Y. Huang, Y. Fan and W. Du: "Static Voltage Sharing Design of a Sextuple-Break 363 kV Vacuum Circuit Breaker", Energies 2019, 12, 2512, June 2019.
[9] S. Ai, X. Yu, Y. Huang, F. Yang, Y. Fan, X. Li: "Voltage Distribution Design of a Novel 363 kV Vacuum Circuit Breaker", 2018 IEEE International Conference on High Voltage Engineering and Application (ICHVE), Athens, Greece, September 2018.
[10] N. Ide, O. Tanaka, S. Yanabu, S. Kaneko, S. Okabe, Y. Matsui: "Interruption Characteristics of Double-Break Vacuum Circuit Breakers", IEEE Transactions on Dielectrics and Electrical Insulation, Vol. 15, No. 4, August 2008, pp. 1065-1072.
[11] T. Fugel, D. Koenig: "Influence of Grading Capacitors on the Breaking Performance of a 24-kV Vacuum Breaker Series Design", IEEE Transactions on Dielectrics and Electrical Insulation, Vol. 10, No. 4, August 2003, pp. 569-575.
[12] S. Giere, H. Knobloch, J. Sedlacek: "Double and Single-Break Vacuum Interrupters for High Voltage Application – Experiences on Real High-Voltage Demonstration-Tubes", 39th Cigré Session, 13-202, Paris, France, August 2002.
[13] B. Blez, C. Guilloux: "Post-Arc Current in High Voltage SF6 Circuit-Breakers at up to 63 kZ", IEEE Power Engineering Review, Vol. 9, No. 4, April 1989, pp. 64-65.
[14] R. P. P. Smeets, V. Kertész, D. Dufournet, D. Penache, M. Schlaug: "Interaction of a Vacuum Arc with an SF6 Arc in a Hybrid Circuit Breaker During High-Current Interruption", IEEE Transactions on Plasma Science, Vol. 35, No. 4, August 2007, pp. 933-938.
[15] K. Steinke, M. Lindmayer, K.-D. Weltmann: "Post-Arc Current of Vacuum Interrupters with Axial Magnetic Field Contacts under High Current and Voltage Stress", 19th International Symposium on Discharges and Electrical Insulation in Vacuum (ISDEIV), Xi'an, China, September 2000.
[16] W. Haas, N. Wenzel: "Das Nachstromverhalten stromstarker Metalldampf-Lichtbögen in Vakuum", Siemens AG, Zentralabteilung Forschung und Entwicklung, 1996.
[17] S. Yanabu, M. Homma, E. Kaneko, T. Tamagawa: "Post Arc Current of Vacuum Interrupters", IEEE Transactions on Power Apparatus and Systems, Vol. PAS-104, No. 1, January 1985, pp. 166-172.